Human Molecular Genetics, 2004, Vol. 13, No. 16 ***1763–1773***
doi:10.1093/hmg/ddh192
Advance Access published on June 30, 2004

Molecular analysis of the genetic defect in a large cohort of IP patients and identification of novel *NEMO* mutations interfering with NF-κB activation

Francesca Fusco[1,†], Tiziana Bardaro[1,†], Giorgia Fimiani[1], Vincenzo Mercadante[1], Maria Giuseppina Miano[1], Geppino Falco[1], Alain Israël[2], Gilles Courtois[2,‡], Michele D'Urso[1] and Matilde Valeria Ursini[1,*]

[1]Institute of Genetics and Biophysics, Adriano Buzzati Traverso-CNR, Naples, Italy and [2]Unité de Biologie Moléculaire de l' Expression Génique, Institut Pasteur, Paris, France

Received April 8, 2004; Revised May 25, 2004; Accepted June 11, 2004

Incontinentia Pigmenti (IP) is an X-linked genodermatosis that is lethal for males and present in females with abnormal skin pigmentation and high variable clinical signs, including retinal detachment, anodontia, alopecia, nail dystrophy and nervous system defects. The NF-κB essential modulator (*NEMO*) gene, responsible for IP, encodes the regulatory subunit of the IκB kinase (IKK) complex required for nuclear factor κB (NF-κB) activation. We analyzed the *NEMO* gene in 122 IP patients and identified mutations in 83 (36 familiar and 47 sporadic cases). The recurrent *NEMO* exon 4–10 deletion that is the major cause of the disease was present in 73 females (59.8%). In addition 10 point alterations (8.2% of females) were identified: three frameshift, three nonsense, three missense and one in-frame deletion of a single amino acid. We measured the effects of these *NEMO* point-mutations on NF-κB signaling in *nemo*(−/−) deficient murine pre-B cells. A mutation in the N-terminal domain, required for IKK assembly, reduced but did not abolish NF-κB activation following lipopolysaccharide stimulation. Mutations that disrupt the C-terminal domain, required for the recruitment of upstream factors, showed lower or no NF-κB activation. A phenotype score based on clinical features of our IP patients was applied for summarizing disease severity. The score did not correlate with mutation type or domain affected indicating that other factors influence the severity of IP. Such a factor is likely to be X-inactivation. Indeed, 64% of our patients have extremely skewed X-inactivation pattern (≥80:20). Overall IP pathogenesis thus depends on a combination of X-inactivation and protein domain that recruit upstream factors and activate NF-κB.

INTRODUCTION

Incontinentia Pigmenti (IP) is a rare X-linked dominant genodermatosis, lethal for males during embryogenesis. Heterozygous females can instead survive owing to X-inactivation mosaicism. Abnormal skin pigmentation, retinal detachment, anodontia, alopecia, nail dystrophy and nervous system defects are all characteristic signs of IP (1). Currently, early diagnosis of IP is based on the presence of abnormal skin pigmentation that evolves in four dermatological stages. Again on the basis of X-chromosome mosaicism selection, it disappears by the second decade and adults may retain only areas of dermal atrophy.

The gene responsible for IP encodes the 48 kDa NF-κB essential modulator (NEMO) protein, also referred to as IKKγ, which is the essential modulator of nuclear factor κB (NF-κB) (2,3). NEMO serves as a scaffolding subunit that binds two proteins with kinase activity (IKKα and IKKβ), necessary for NF-κB activation (4). In resting cells, NF-κB homo- and heterodimers are sequestered in the cytoplasm through

*To whom correspondence should be addressed. Email: ursini@igb.cnr.it
†The authors wish it to be known that, in their opinion, the first two authors should be regarded as joint First Authors.
‡Present address: INSERM U532, Hôpital Saint-Louis, Paris, France.

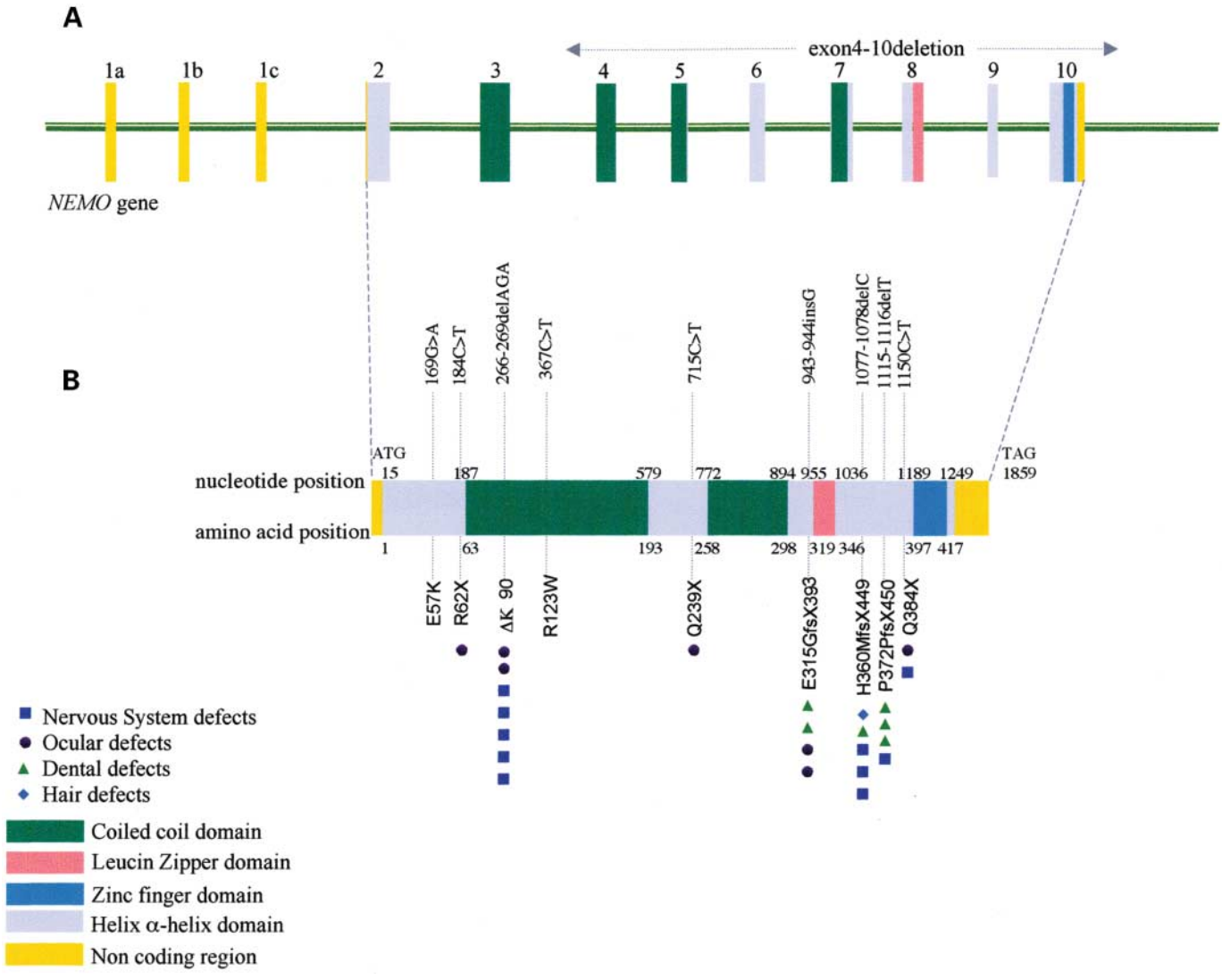

Figure 1. (**A**) The exon–intron *NEMO* gene structure. **(B)** Summary of the *NEMO* mutations detected in this study and in Aradhya *et al.* (mutation E57K, R62X) (15). Black symbols represent the clinical signs of each mutated NEMO patient as described in the legend.

interaction with one or more inhibitory proteins, the IκBs. After stimulation by many known stimuli, IκB is phosphorylated by the IκB kinase (IKK) complex and promptly degraded by the ubiquitin–26S proteasome pathway (5,6). NF-κB then can shuttle to the nucleus, where it activates target-gene transcription. NEMO contains two coiled-coil motifs (CC1 and CC2) and a leucine zipper (LZ) domain, required for IKKα–IKKβ association and its oligomerization, and a zinc finger (ZF) domain at the C-terminus required for the recruitment of upstream factors but not for complex assembly (2,3). NEMO is known to be the only subunit absolutely required for the activation of the IKK complex, but only some features of its action are well understood. Thus, it appears that NEMO is the point of convergence for many NF-κB activation pathways, including those induced by TNF-α, IL-1, lipopolysaccharide (LPS) or other proinflammatory cytokines and by dsRNA (4,6).

nemo-deficient mice recapitulate features of human IP disease (7–9). Male mutant mice die prenatally, even earlier than other mice with mutated NF-κB signaling proteins, because of dramatic liver degeneration due to TNF-α induced hepatocyte apoptosis. Female mice develop IP-like skin lesions with granulocyte infiltration, hyperkeratosis and increased apoptosis. Although many female mice die during these inflammatory stages, some survive and are fertile. The death and clearance of *nemo*-deficient cells probably account for this recovery.

Additional genetic studies revealed that IP is allelic with an X-linked immunodeficiency syndrome termed hypohidrotic ectodermal dysplasia with severe immunodeficiency (EDA-ID), which, unlike IP, is associated with specific developmental and immunological defects in males (10). It was proposed that loss-of-function mutations in *NEMO* were associated to IP, whereas *NEMO* hypomorphic mutations, which did not severely reduce NF-κB activation, were associated with EDA-ID (10–12).

Owing to the ubiquitous nature of the NF-κB pathway, clinical manifestations of IP show a large phenotypic range,

from simple cutaneous manifestations to neurological problems. The signaling pathways that lead to activation of NF-κB via the IKK complex differ among tissues, and may use different mechanisms to activate NEMO. The availability of natural *NEMO* mutants should therefore provide important clues about its functions and the molecular mechanism that leads to IP. Previous data reported by us and others (13–15) revealed that an identical genomic deletion within NEMO account for the majority of identified mutations and that the remaining mutations are small duplications, substitution or deletion, scattered all along the gene. However, most of the small mutations previously described produce early truncated NEMO protein, precluding any analysis of the correlation between the protein domain affected, the efficiency of the NF-κB activation process and the phenotype presentation (15).

Here, we report a mutational analysis of the *NEMO* gene in a large, clinically well characterized cohort of 122 unrelated IP patients. We measured the effects of these *NEMO* point-mutations on NF-κB signaling in *nemo*-deficient murine pre-B cells. A phenotype score was also applied to the clinical feature of our IP patients, and skewed X-inactivation pattern in their peripheral blood cells was measured. *NEMO* mutations we have isolated in this study account for the majority but not all clinical cases; moreover, the detected mutation spectrum do not allow genotype–phenotype correlation, leading to the hypothesis that other factors may modulate the IP pathogenesis.

RESULTS

NEMO mutations in IP patients

We performed a mutational analysis of *NEMO*, a 23 kb gene composed of 10 exons (GenBank accession no. AJ271718) (13) (Fig. 1), in a cohort of 122 patients diagnosed with IP. We found a recurrent *NEMO* deletion (exons 4–10) in 73 out of 122 patients (59.8%) using the polymerase chain reaction (PCR) test as described by Bardaro *et al.* (14) (Table 1). Among these, 39 (53%) appeared to be *de novo* mutations in isolated cases with no family history of IP.

In 49 (40.2%) IP patients that did not show the recurrent deletion, denaturing high performance liquid chromatography (DHPLC) analysis of all coding exons (exons 2–10) revealed 10 point-mutations in 10 unrelated patients (8.2%) (Table 2). Sequence tracings of the described mutations and all the pedigrees are shown in Figure 2. Seven of them were sporadic cases suggesting that the mutations were generated as *de novo* alterations. DNA analysis of parents of IP females revealed abnormalities in only three cases: the mother of patient 1-SA (E57K), the mother of patient 4-PB (R123W) and the mother of patient 8-MF (E315GfsX393). These mothers showed only mild dermatological signs, compatible with diagnosis of IP. Among the 10 small nucleotide changes, eight of them had not been described previously. Specifically, three are missense mutations (E57K, D113N and R123W in patients 1-SA, 3-LE and 4-PB, respectively), three are nonsense mutations (R62X, Q239X and Q384X in patients 5-SE, 6-RE and 7-TE, respectively), one is a single-nucleotide insertion (E315GfsX393 in patient 8-MF), two are single-nucleotide deletions leading to frameshift (H360MfsX449 and P372PfsX450 in patients 9-SA and 10-CL, respectively) and one is an in-frame deletion of a codon resulting in one amino acid microdeletion (ΔK90 in patient 2-DA). We subdivided these *NEMO* point-mutations in different groups, according to their effect on the predicted protein (NCBI ORF finder, Fig. 3). The first class comprises mutations affecting the N-terminal and CC1 domains (group A) (Fig. 3, protein translations 1–4). Specifically, the patient 1-SA carries a transition 169G → A (E57K) that was already described (15); the patient 2-DA carries an in-frame

Table 1. Summary of the clinical data of IP patients carrying the classical *NEMO* Δexon4–10 deletion

Patient	Nervous system	Ocular defects	Dental defects	Hair defects	Nail defects	Phenotype score
11-AA	0	0	0	0	0	0
12-AP	0	0	0	1	0	1
13-ASC	0	0	0	1	0	1
14-BL	0	0	0	0	0	0
15-BP	0	2	4	1	1	8
16-BJ	0	0	0	0	0	0
17-BVR	0	0	1	0	0	1
18-BK	0	1	1	0	0	2
19-CG	0	0	3	0	0	3
20-CV	0	0	0	0	0	0
21-CA	0	0	0	0	0	0
22-DL	0	0	0	0	0	0
23-DBF	0	0	1	1	0	2
24-DLD	0	0	0	0	1	1
25-DL	0	0	2	0	0	2
26-FG	0	0	1	1	0	2
27-FL	0	0	1	0	0	1
28-FC	2	0	0	0	0	2
29-GAF	0	0	0	0	0	0
30-GC	0	0	0	0	0	0
31-GSC	0	0	0	0	0	0
32-GJB	0	0	0	0	0	0
33-GEB	0	0	2	1	2	5
34-GMC	0	0	3	0	0	3
35-LC	0	0	0	0	0	0
36-LJ	0	0	0	0	1	1
37-LM	0	0	0	0	0	0
38-LFM	0	0	0	0	0	0
39-LSM	0	0	1	0	0	1
40-MF	3	0	3	0	0	6
41-MM	0	0	1	0	1	2
42-ML	0	0	0	0	0	0
43-MM	0	1	2	0	2	5
44-MA	0	0	1	0	0	1
45-PG	2	2	1	1	0	6
46-PM	0	0	0	0	0	0
47-PR	1	1	2	0	0	4
48-PA	0	0	1	0	0	1
49-PGM	0	1	0	0	0	1
50-RG	0	0	0	0	0	0
51-RTB	0	1	2	0	0	3
52-RO	0	0	4	1	0	5
53-SM	0	0	0	0	0	0
54-SV	0	0	0	0	0	0
55-SG	0	0	0	0	0	0
56-TZ	0	0	0	0	0	0
57-TC	0	0	1	0	0	1
58-VI	0	0	0	0	0	0
59-WC	0	1	2	0	1	4
60-ZE	0	0	0	0	0	0
Total %	8%	16%	44%	16%	14%	

Table 2. Summary of the clinical data of IP patients carrying a *NEMO* point-mutation. Phenotype score was calculated for each tissue involved in IP. Percentages of patients carrying defects in each tissue are indicated

Patient	Nucleotide change	Nervous system	Ocular defects	Dental defects	Hair defects	Nail defects	Phenotype score
		Seizures Spastic paresis Motor and mental retardation Microcephaly	Strabismus Cataracts Optic atrophy Retinal vascular pigmentary abnormalities Microphthalmous	Partial anodontia Delayed dentition Cone/peg shaped teeth Impactions	Vortex alopecia Wooly hair naevus Eyelash and eyebrow hypogenesis	Onycho gryphosis Pitting Ridging	
1-SA	169G → A	0	0	0	0	0	0
2-DA	266–269delAGA	5	2	0	0	0	7
4-PB	367C → T	0	0	0	0	0	0
5-SE	184C → T	0	1	0	0	0	1
6-RE	715C → T	0	1	0	0	0	1
7-TE	1150C → T	1	1	0	0	0	2
8-MF	943–944insG	0	2	1	0	0	3
9-SA	1077–1078delC	3	0	1	1	0	5
10-CL	1115–1116delT	1	0	3	0	0	4

deletion of a triplet (266–269delAGA) (ΔK90) leading to a microdeletion of a lysine residue at position 90 of the protein; in patient 3-LE we have observed a transition 337G → A (D113N) that appeared to be a conservative substitution, because it was observed in one out of 120 female controls. The patient 4-PB showed a transition 367C → T (R123W). Both the 367C → T (R123W) transition and the 266–269delAGA (ΔK90) are located in the CC1 domain and may affect the IKK complex assembling. Of note, the arginine residue at codon 123 (R), the lysine residue (K) at codon 90 and the glutamic acid at codon 57 are all evolutionarily conserved positions (data not shown).

The second group (group B, Fig. 3, protein translations 5–7) contains proteins lacking portion of the C-terminal domain. More specifically, the 184C → T (R62X) transition identified in patient 5-SE [already reported elsewhere (15)], causes a complete loss of function of NEMO protein. The 715C → T (Q239X) and 1150C → T (Q384X) transitions identified in patients 6 and 7, introduce premature stop codons immediately upstream of the CC2 and ZF domains, respectively.

Mutations described in the group C (Fig. 3, protein translations 8–10) include two frameshift mutations that alter only the LZ and the ZF domains, producing proteins with complete CC1 and CC2 domains but lacking the LZ and ZF (shorter protein, translation 8) or complete CC1/2 and LZ domains (elongated protein, translations 9 and 10). The 943–944insG (E315GfsX393), identified in the patient 8-MF, causes a frameshift that leads to a mutated LZ domain and completely removes the putative ZF domain located at the extreme C-terminus of the NEMO protein. Two small deletions (1077–1078delC, 1115–1116delT) within the same region upstream the ZF domain causes a frameshift and a premature stop codon 89 and 78 in patients 9-SA and 10-CL, respectively.

We identified mutations in 83 of 122 cases with classical IP (32%). In addition, we analyzed the *NEMO* coding region, but neither changes in the promoter region nor large DNA rearrangement or deletions were assessed. Gross gene deletions and rearrangements have been commonly observed in patients with other X-linked diseases such as Duchenne muscular dystrophy and haemophilia A (16,17). Therefore, although locus heterogeneity remains a possibility in IP, any other gene(s) involved would only account for a minor proportion of classical IP cases.

Functional analysis of *NEMO* mutations

To investigate the functional relevance of the small *NEMO* mutations reported here, we used a cis-reporter luciferase plasmid that provides a simple and rapid assessment of the *in vivo* activation of the NF-κB pathway. The reporter pIgk-Luc plasmid expresses the luciferase gene downstream three NF-κB binding sites. We used site-directed mutagenesis to generate recombinant plasmids containing *NEMO* cDNAs carrying each of the nine small mutations isolated in our IP cohort (only R62X was not included in the analysis) in the pcDNA3 vector. We examined the ability of these NEMO mutants to restore the NF-κB activation in reconstituted mouse 1.3E2 cells [*nemo*$^{-/-}$ murine pre-B lymphocytes (18)], measuring the luciferase activity, after LPS stimulation. LPS is the principal component of Gram-negative bacterial wall, which activates the innate immune system inducing the NF-κB pathway via the Toll-like receptors (19). The luciferase activity generated by the ΔK90 mutation, affecting the CC1 domain, was only 46.3% of the activation obtained with NEMO WT protein, whereas NEMO E57K, NEMO D113N and NEMO R123W showed the same luciferase activity as the control (Fig. 2; protein activity column). In contrast, the mutations eliminating the CTS domain (Q239X, E315GfsX393 and H360MfsX449) exhibited little or no NF-κB activation (0, 0 and 3.4%, respectively). Only the Q384X mutation, that preserves the complete CC2 and LZ domains, retained 37.5% of the NEMO WT activation.

Interaction of the mutant NEMO protein in the IKK complex

We examined whether IKKα and IKKβ could still physically interact with the mutant NEMO proteins. In particular, we

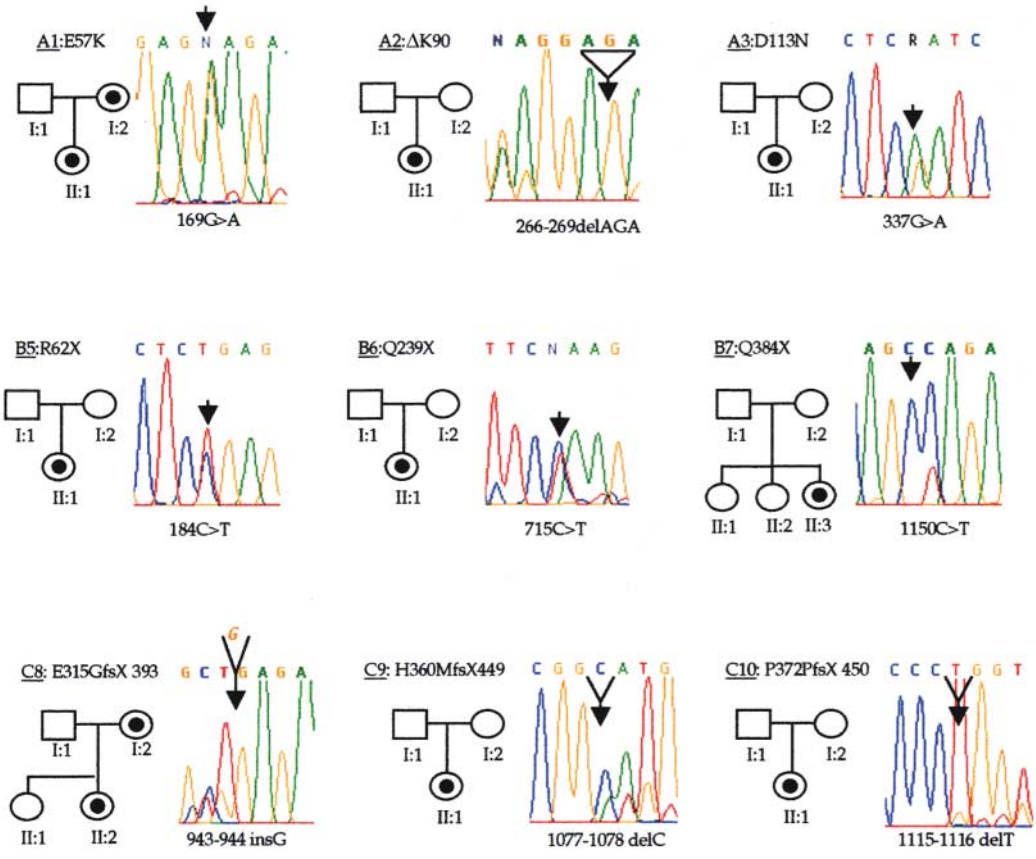

Figure 2. Pedigree informations and respective mutations in IP families.

tested the ability of two mutations falling in the coiled-coil domain 1, ΔK90 and D113N, to associate with IKKs. HEK 293T cells were cotransfected with combinations of the empty vector (pcDNA3) or ΔK90 and D113N constructs with either FLAG–IKKα or FLAG–IKKβ plasmids. Cell extracts were immunoprecipitated with an anti-FLAG antibody and then analyzed by immunoblotting assay with an anti-NEMO (Fig. 4).

We found that IKKβ immunoprecipitation brought down less ΔK90 mutant protein compared with WT NEMO, consistent with the ΔK90 mutant having lower affinity for IKKβ, whereas the amount of immunoprecipitated D113N was perfectly comparable with the amount of immunoprecipitated WT NEMO (Fig. 4B). These results confirm that D113N is a polymorphic functional variant of the NEMO protein. Interestingly, the same kind of experiment performed using a FLAG–IKKα did not reveal any defect in the amount of immunoprecipitated ΔK90 NEMO, suggesting that the observed defect was IKKβ specific (Fig. 4A).

Genotype–phenotype correlation

Comprehensive phenotype data were available on a total of 60 IP patients, 50 of which carrying genomic deletion and 10 with point-mutations. We evaluated the clinical features and correlated the mutation type with clinical traits involving NS, eyes, teeth, hair and nails that, indeed, are the most frequent pathological signs observed among IP patients. Moreover, all tissues involved in IP are derived from the neural crest and thus have the same neuroectodermal derivation. The abnormal skin pigmentation, that was present in all patients, was not included. On the basis of the clinical data, a phenotypic severity score was calculated for each patient, summarizing the pathologic clinical features (Tables 1 and 2). Patients carrying mutations ΔK90 and H360MfsX449 (Table 2, patients 2-DA and 9-SA, respectively) have been found to have higher values for the combined score (score 7 and 5, respectively) and therefore suffered more severe disease than patients with missense mutations (score 0 for 1-SA, E57K, and 4-PB, R123W) or those with a nonsense mutation (score 0 for 6-RE, Q239X and 2 for 7-TE, Q384X). Moreover, the patient 10-CL, carrying the mutation P372PfsX450 showed a phenotype score of 4. High variability of the phenotype scores was observed in patients carrying the mutation Δexon4–10 (Table 1). Eleven patients (22%) showed a very high score (score 3–8); six (12%) showed two clinical features combination (score 2); 33 (66%) had one pathologic character (score 1) or showed only abnormal skin pigmentation (score 0). Nervous system defects were observed in 44% of patients carrying point-mutations and ocular defects in 55% of patients, whereas only 8% of IP patients with genomic deletion suffered nervous system defects and 16% had ocular defects.

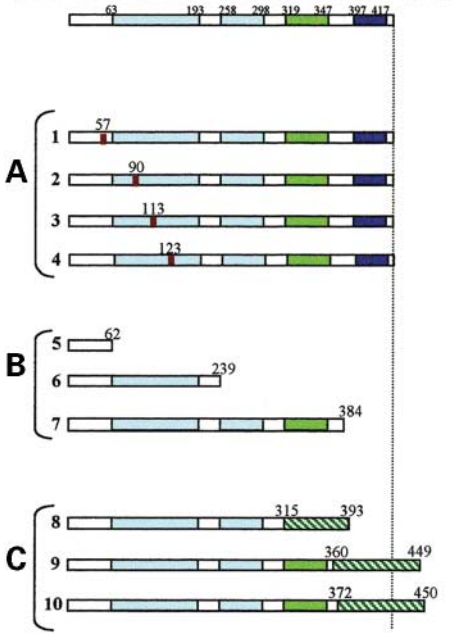

	Aminoacid change[a]	Affected domain	Nucleotide change	Exon involved	Protein activity[b] (% of control)	Phenotype score	X-inactivation in PBL
	Wild-type	/	/	/	100	/	
A 1	E57K	NTS	169G>A	2	100	0	67%
A 2	ΔK90	CC1	266-269delAGA	3	46.3	7	73%
A 3	D113N	CC1	337G>A	3	100	0	99%
A 4	R123W	CC1	367C>T	3	100	0	64%
B 5	R62X	NTS	184C>T	2	0	1	100%
B 6	Q239X	CTS	715C>T	6	0	1	60%
B 7	Q384X	ZF	1150C>T	10	37.5	2	65%
C 8	E315GfsX 393	CTS	943-944insG	8	0	3	97%
C 9	H360MfsX 449	ZF	1077-1078delC	9	3.4	5	99%
C 10	P372PfsX 450	ZF	1115-1116delT	9	n.t.	4	54%

Figure 3. *NEMO* point-mutation groups and their functional effect. The predicted protein translations are shown for the different mutations at the left. Predicted missense mutations (group **A**, protein translations 1, 3, 4) and an in-frame deletion (group A, protein translation 2). Nonsense mutations (group **B**, protein translations 5–7). Frameshift mutations leading to elongated proteins with complete N-terminal domain (group **C**, protein translation 8–10). The cyan boxes indicate the CC domains; green box shows the LZ domain and blue box indicates the ZF domain. The green diagonal strips represent those areas of the protein that, because of a frameshift mutation, are translated differently to the normal NEMO protein. [a]Numbered from the ATG initiator codon according to Smahi A. (13); [b]Protein activity is obtained in a complementation assay. NTS, N-terminal sequence; CTS, C-terminal sequence; CC1, coiled-coil domain 1; LZ, leucine zipper domain; fs, frameshift; stop, stop codon; PBL, peripheral blood leucocytes. n.t., no tested.

X-Inactivation studies

X-Inactivation studies were performed on peripheral blood of 53 IP patients. The age of patients included in this analysis was restricted to those of 25 years of age or younger, as skewing is known to increase with age (20,21). Using the androgen receptor (AR) X-inactivation assay, we determined the X-inactivation pattern of all female subjects (41 carrying the Δexon4–10 deletion, 12 point-mutations, including three carrier mothers). The frequency of X-inactivation pattern for single classes of value is shown in Table 3. An X-inactivation pattern $<80:20$ is demonstrated in $\sim$100% of control females, which is generally consistent with previous estimations (22). In contrast, 64.1% of IP patients show X-inactivation patterns that were $\geq 80:20$ (Table 3) and 45.3% have X-inactivation values $\geq 90:10$%. Totally, 31 of these patients have Δexon4–10 mutation and three have a point-mutation. We also examined the X-inactivation pattern in peripheral blood of three families each having a daughter carrying a point-mutation (E57K, R123W and E315GfsX393). All the mothers have the same mutation as their daughters and show a moderately skewed X-inactivation profile. Furthermore, we tested the X-inactivation pattern in the sister of the patient with the point-mutation E315GfsX393 and we found it is severely skewed (97 : 3%).

DISCUSSION

Mutations in *NEMO* gene are the primary cause of IP

In this study, we have analyzed the coding region of the *NEMO* gene in 122 unrelated IP patients, finding pathogenic mutations in 83 of them (68%). Mutations in *NEMO* are thus the primary cause of IP (2,3). Patients that lack of mutations in the coding region may have mutations in regulatory regions that have not yet been analyzed.

Totally 87.9% (73 of 83 patients carrying mutations) of our patients have an identical genomic deletion from exon 4 to 10. This large deletion results from slipped mispairing between two identical MER67B repeated sequences (13). The remaining 12.1% of the mutations found in our patients are small nucleotide substitutions, deletions and insertions (15). Only one missense mutation was identified as a conservative substitution (D113N patient 3-LE Fig. 2). Among the 122 IP patients analyzed here, 47 were sporadic cases.

As previously reported (15), small mutations are scattered along the *NEMO* gene, consistent with the importance of the entire NEMO protein sequence for its function. Interestingly, all the single-nucleotide substitutions are C → T transitions (or G → A when the 5-methylcytosine deamination occurs on the antisense strand), three of them occurring at CpG sites.

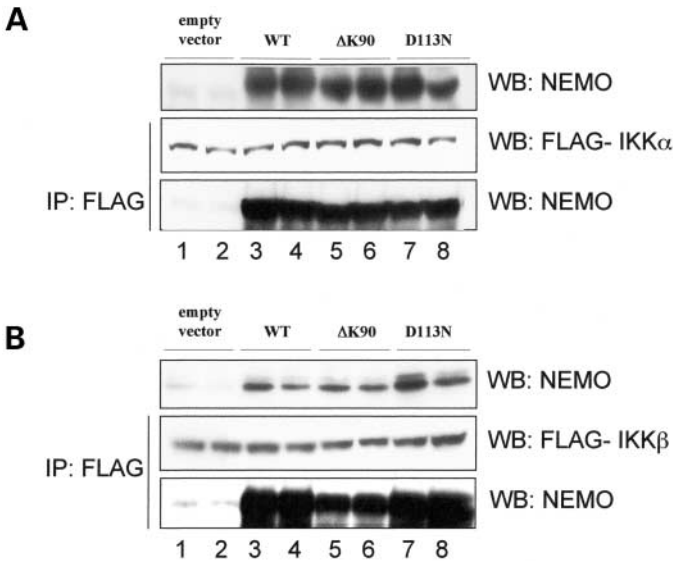

Figure 4. Interaction between NEMO wt or variants and IKK subunits. (**A**) NEMO–IKKα interactions. HEK 293T were transfected with FLAG–IKKα (lanes 1–8) together with empty vector (lanes 1 and 2), NEMO wt (lanes 3 and 4), ΔK90 (lanes 5 and 6) or NEMO D113N (lanes 7 and 8). Co-immunoprecipitation of NEMO molecules with IKKα was detected with a specific anti-NEMO antibody after immunoprecipitating IKKα with anti-FLAG. (**B**) NEMO–IKKβ interactions. Same as in (A) except that FLAG–IKKβ was used instead of FLAG–IKKα.

They were probably caused by methylation of a cytosine residue to 5-methylcytosine that predisposes by spontaneous deamination to thymidine. In many cases germ-line CpG transition mutations show a male predominance (23), and we hypothesized that the majority of *de novo NEMO* mutations described here leading to IP arise from 5mC → T deamination in male germ cells. Previous reports have indicated a 2-fold increase in male germ cells occurrence of new IP mutations (10/5 male : female ratio), and a high male : female ratio of germ-line mutations has been measured in other X-linked genetic disorders such as haemophilia A and B (23,24), and suggested for Rett syndrome (25). On the basis of the high *de novo* mutation rate reported here, we suspect that the prevalence of IP (1 : 10 000/20 000) is underestimated.

Functional analysis of NEMO mutants

We analyzed the effect of the *NEMO* mutations on NF-κB activation, using LPS as a stimulus. Three NEMO mutant polypeptides lack the putative ZF domain, located at the C-terminal extremity, that is required for the binding of the IKK complex to upstream activators and for the subsequent NF-κB activation. In two of them (H360MfsX449 and P372PfsX450), a frameshift mutation causes the production of polypeptides longer than the WT (the wild-type protein is 417 amino acids, whereas these mutated protein are 449 and 450 amino acids, respectively). We have evaluated the functional consequences of H360MfsX449 that severely impaired NF-κB activity (3.4%). The third predicted mutant polypeptide (Q384X), truncated at codon 384, restore 37.5% of the WT NF-κB activity. The different extent of NF-κB activation

Table 3. X-Inactivation patterns in IP patients and in control subjects

Frequency of skewed X-inactivation			
X-inactivation pattern	Female control subjects ($n = 17$)	*NEMO* Δexon 4–10 carriers ($n = 41$)	*NEMO* point mutations carriers ($n = 12$)
≥90 : 10	0	21 (51.3)	3 (25)
≥80 : 20	0	10 (24.4)	0
≥70 : 30	3 (17.6)	3 (7.3)	2 (17)
≥60 : 40	6 (35.3)	3 (7.3)	6 (50)
≥50 : 50	8 (47)	4 (9.7)	1 (10)

observed between the different types of mutants without ZF (from 37.5 to 0%) may result from decreased stability of the NEMO polypeptides with incorrect amino acid sequences.

The two mutations that disrupt both LZ and ZF domains produce a protein truncated at position 239 or a protein with frameshift from position 315 (Q239X and E315GfsX393). These products did not show any detectable LPS induction *in vitro* (Fig. 3). The impaired NF-κB activation could be due to the inactive NEMO protein and also due to reduce *NEMO* mutant expression.

The four missense mutations found in our cohort of IP patients all fall in the CC1 domain and could affect a region required for binding IKKα and IKKβ into a high-molecular weight complex essential for kinase activity. D113N is a conservative substitution and, in fact, rescues 100% of the NF-κB activity. Of the remaining three mutations, only ΔK90 exhibited a reduced NF-κB activation (46.3%) in our luciferase assay, based on the use of LPS as the stimulus. E57K and R123W may nevertheless be defective in other signaling pathways, such as the one used by IL-1 or TNF-α. Concerning IL-1, this is unlikely, as this cytokine acts through a receptor that recruits the same signaling molecules as TLR4, the LPS receptor (19). In the case of TNF-α, the analysis cannot be done using 1.3E2 mutant cells as the wt cells they are derived from, 70Z/3, lack TNF-R expression (26). To analyze this pathway, and others that may contribute to the IP disease, we are currently trying to use other NEMO(−) cells, such as NEMO(−) MEFs (9).

Mutations in different domains of the NEMO protein could also affect interaction with tissue-specific intracellular transducers and thus produce tissue-specific defects. Indeed, evidence is emerging that NF-κB pathway has a critical role in CNS in processes such as neuronal plasticity, neuro-degeneration and neuronal development (27). In this respect it is noteworthy that, most of the mutations described here are associated with severe NS and ocular defects including seizure, mental retardation and microcephaly, which are generally considered as developmental defects (28,29).

A critical role for NEMO activity is in the formation of functional IKK complex. Interestingly, ΔK90 NEMO, which lacks a residue presumably involved in IKK complex assembly, still retains the ability to interact with IKKα but exhibit a reduced interaction with IKKβ. As it has been shown that NEMO interacts with both IKKα and IKKβ̃, but that the two catalytic subunits do not play the same role *in vivo*, the ΔK90 NEMO protein might generate a shift from IKKα–IKKβ–NEMO complexes to IKKα–IKKα–NEMO complexes, which

would disturb the NF-κB activation process. We are in the process of generating cells stably expressing ΔK90 to verify this hypothesis.

In summary, *NEMO* mutations described here affect the NF-κB activation after LPS triggering. However, this effect is much more evident in C-terminal disease-linked mutations producing truncated protein than in N-terminal disease-linked mutations, which are mainly missense changes that only slightly affect the NF-κB activity. This is in agreement with the previously reported *in vitro* data on NEMO functional analysis, which suggested that the C-terminus of NEMO protein contains interaction domains that are absolutely required for connecting the IKK complex to the upstream activators (3).

The relevant incidence of hypomorphic mutations found in our IP patient cohort (11%) somewhat modifies the general assumption that IP is caused only by *NEMO* loss-of-function mutation. In addition, many of the mutations responsible for IP map near to the mutations identified in EDA-ID patients (12), which mainly affect the C-terminal domain. Thus, similar mutation can cause two clinically distinct diseases: EDA-ID in hemizygous males and IP in heterozygous females.

Genotype–phenotype correlation and X-inactivation analysis in IP patients

A phenotype scoring system was used for examining correlation between the mutation type and the clinical presentation of IP patients. To assess genotype–phenotype correlation in IP patients, we listed features that are typical for IP but not consistent in all patients and could therefore reflect the severity of the syndrome (Tables 1 and 2). For calculating the score we included only defects relative to nervous system, eyes, teeth, hair and nail, that are most frequently, but not always, observed in IP patients. We did not include in the score calculation abnormal skin pigmentation, that is present in all patients. If a genotype–phenotype correlation does exist, females who carry loss-of-function mutations would be expected to have the most severe phenotype. In our study, however, this is not the case: 50 patients with the same exon 4–10 *NEMO* deletion have severity score ranging from 1 to 8. In addition, at the milder end of the spectrum we would expect to find patients who carry missense mutations that only slightly affect NEMO function. Patient 1-SA (E57K) fulfils these criteria, indeed she has a mild phenotype (score 0). In contrast, patient 2-DA (ΔK90) is severely affected (score 7). We have also documented cases of females carrying the same point-mutation but presenting a different clinical picture (patient 8-MF, pedigree in Fig. 2). Factors that may influence the phenotype include the X-inactivation pattern.

To get insights about the X-inactivation status we measured skewing in peripheral blood lymphocytes (PBL) from 52 patients. In general, the observed incidence of skewing in our cohort of IP patients is 76.4%, higher than would be expected in a normal population with a maximum age of 25 (20,21). A higher degree of skewing (100%) has been observed in association with the common rearrangement as well as with the truncating mutation (R62X), which causes loss-of-function of NEMO, whereas for the mutations that still retain some activity, such as ΔK90 and Q384X, the X-inactivation value decreased (73 and 65%, respectively). We hypothesize that cells expressing the mutation that preserves some NEMO activity (hypomorphic mutations) may still be partially active early after the X-inactivation process and would survive while cells expressing loss-of-function *NEMO* mutations would disappear preferentially after X-inactivation. This would also explain the high prevalence of skewed X-inactivation observed in IP patients with loss-of-function or early truncating mutations (Fig. 3 and R62X). The case of the female patient carrying the D113N polymorphic NEMO variant deserves particular attention, as it has full functional activity and was found to be 99% skewed. We may hypothesize that this patient is also carrying an additional NEMO mutation (rearrangement, mutation in regulatory regions, etc.) escaping from our molecular analysis but causing the skewed X-inactivation.

We also found that mutations preserving some activity show an atypical phenotype characterized by involvement of much more tissues than classical IP phenotype. This is true for ΔK90 and for the two frameshift mutations at the C-terminal end of the NEMO protein, 1077–1078delC and 1115–1116delT (score 5 and 4, respectively). Those NEMO mutations are associated with more severe NS and ocular defects than those associated with exon 4–10 deletion mutation. Hypomorphic mutations thus may have broader phenotypic consequence than typical IP, in which skewed X-inactivation is likely to modulate the severity of the disease. Aradhya *et al.* (15) proposed this same interpretation of the data on the basis of a molecular analysis of NEMO mutation in a large cohort of IP patients. However, in that case phenotypic variability of IP presentation was not corroborated by functional data as the spectrum of mutations described there included most mutations prematurely disrupting NEMO protein.

In summary, although X-inactivation is likely to play a role in modulating the pathogenic effects of different mutations, the X-inactivation performed on PBL cannot allow us to draw any conclusion about the skewed X-inactivation in other tissues that show pathological sign. However, PBL serve as a phenotypic surrogate for cells in the affected tissue as for example central nervous system, eye, etc. Accordingly, NEMO mutants associated with skewing might affect *in vivo* cell viability and proliferation in many tissue types including PBL. We hypothesize that IP may arise precisely in those cells that survive with partial NEMO function, as in developing brain after early neuronal plasticity is lost. This is in contrast with those cases in which the NEMO activity is absent, where dysfunctional cells are lost and their function is taken over by their WT neighbors. The variability in IP phenotypes would then result from a combination of the type of mutation, the functional domain affected and X-inactivation.

MATERIALS AND METHODS

Patients

All the IP patients we analyzed in this study met the 1993 revised criteria for classification of IP (1). All patients' material was gathered, after receiving informed consent from participants, under protocols approved by the Declaration of

Helsinki. Each potential participant with IP was interviewed and asked to complete an extensive questionnaire. Only 60 questionnaires were available. All medical records of IP-affected family members were reviewed to confirm the diagnosis. The affected females had a history of perinatal blistering and at least one of the other stages of skin lesions. Blood samples were collected in EDTA tubes and genomic DNA was extracted using conventional salt precipitation technique. All patients had an apparently normal karyotype. On the basis of the geographic records of our cohort of IP patients, we established their origins from the following countries: Brazil, Czechoslovakia, Italy, Ireland, Poland, Portugal, Spain, Switzerland, Turkey and UK.

Mutation detection

PCR amplification of IP patients was carried out in a reaction volume of 12 μl with 100 ng of template genomic DNA for each exon with previously reported primers (14). DHPLC analysis was performed according to the manufacturer's protocol (30). Samples showing an abnormal chromatogram were further analyzed by direct sequencing using Big Dye Terminator Cycle Sequencing Reactions on an ABI 3100 (PE Applied Biosystems). Sequence electropherograms were compared with the genomic sequence from GenBank and control samples. Potentially pathogenic changes were validated by DHPLC analysis of 120 normal control females. If the change was not present in control chromosomes, we analyzed samples from IP family members, when available. PCR conditions, primer sequences and DHPLC analysis conditions are available upon request.

To investigate the *NEMO* gene deletion (Δ4–10 exons), a long-range PCR was performed with the EXPAND Long Template PCR system (Roche Mannheim, Germany) according to the manufacturer's protocol. The specific primers for the long-range PCR are reported in Bardaro *et al.* (14).

Mutation nomenclature

Nucleotides were numbered from the first base of the translation initiation ATG codon (BC050612) according to Aradhya *et al.* (15). Mutations were described as recommended by the *ad hoc* committee on mutation (31).

Site-directed mutagenesis and plasmids

The full-length human *NEMO* cDNA was inserted between the *Hind* III and *Not* I sites of the pcDNA3 vector (Stratagene, CA, USA). We generated plasmids carrying the point-mutations found in IP patients using the Quick-change site-directed mutagenesis kit (Stratagene). The sequence of all the mutated constructs was checked by automatic directed sequencing, using T7 and Sp6 primers.The FLAG–IKKβ expression vector (pCMV-F-IKK2) was kindly provided by F. Mercurio (32).

Transfection and complementation assay

The 1.3E2 (*nemo*$^{-/-}$ murine pre-B lymphocytes) cells were grown in RPMI 1640 supplemented with 10% fetal calf serum (FCS) and 50 μM β-mercaptoethanol. The 1.3E2 cells were transiently transfected with the wt NEMO plasmid and all the mutant constructs by a modified DEAE–dextran method described in Courtois *et al.* (18). The following day they were stimulated for 6 h with LPS (Sigma) and finally lysed in a luciferase buffer [25 mM Tris–phosphate (pH 7.8), 8 mM $MgCl_2$, 1 mM DTT, 1% Triton X-100, 15% glycerol]. Luciferase determination was carried out using a Berthold luminometer (Berthold Detection Systems, Germany).

HEK293T cells were grown in DMEM supplemented with 10% FCS. HEK293T cells were transfected using calcium phosphate (33). Briefly, the day before transfection, cells were plated in a 6-multi-well at density of 1.5×10^5 cells in DMEM without FCS. The day after cells were transfected using 1 μg of pcDNA3-NEMOwt, NEMO (ΔK90) or NEMO (D113N) and 1 μg of either pCMV-F-IKKα or pCMV-F-IKKβ. Cells were recovered and cytoplasmic extracts were prepared, 24 h after transfection.

Immunoprecipitations and western blot analysis

Cells extracts from HEK293T were prepared as described elsewhere (2). They were resuspended in 1 ml of TNT buffer [20 mM Tris (pH 7.5), 200 mM NaCl, 1% Triton X-100]. Anti-FLAG (Sigma–Aldrich) was added, and the samples were gently rocked at 4°C for 1 h. A 20 μl volume of protein A–sepharose (Calbiochem, Germany), previously equilibrated in TNT, was added, and the incubation was continued for 30 min. After three washes in TNT (30 s in a microgentrifuge), the beads were resuspended in 1×Laemmli buffer, containing 10% β-mercaptoethanol, and boiled for 5 min. The samples were fractionated on sodium dodecyl sulfate–10% polyacrylamide gels and transferred to nitrocellulose membranes. Western blot was performed using an anti-NEMO antiserum (2) diluted 1:4000 in 0.3% milk/PBS. The IKKα construct was kindly provided by F. Mercurio.

Phenotype analysis

A phenotype score of clinical severity was derived by assessing: (a) a score of 0 in the absence of extracutaneous complications; (b) a score of 1 for nervous system (NS) defects (seizures, spastic paresis, motor retardation, mental retardation or microcephaly); (c) a score of 1 for ocular system defects (strabismus, cataracts, optic atrophy, retinal vascular pigmentary abnormalities, microphtalmous or pseudogliomas); (d) a score of 1 for dental system defects (partial anodontia, delayed dentition, cone/peg shaped teeth or impactions); (e) a score of 1 for hair defects (vertex alopecia, wooly hair naevus or eyelash and eyebrow hypogenesis); (f) a score of 1 for nail defects (onychogryphosis, pitting or ridging). When the score was ≥ 2 for each system/organ the patient suffered by ≥ 2 clinical manifestations for that system/organ. The phenotype severity score allocated represents the addition of the single values of score for each system/organ.

X-Inactivation analysis

XCI patterns in the patients' blood lymphocytes was determined by PCR amplification of the AR locus, a polymorphic region of the X-chromosome containing different numbers of

CAG repeats. The AR locus is consistently methylated on the inactive X-chromosome, making it inaccessible to digestion by the methylation-sensitive restriction enzyme *Hpa* II (New England Biolabs, USA) (34). Genomic DNA from IP patients and from both her parents were digested or not with *Hpa* II. Both digested and undigested DNA were PCR-amplified using primers that amplify a 280 bp product from the *AR* gene. Digestions and PCR were performed as described in Schanen *et al.* (35). The PCR products were separated on an automatic sequencer (MegaBACE^{TM} 1000-Amersham Biosciences, by *BioGeM* gene expression service). The peak heights were calculated according to Hammer *et al.* (36).

ACKNOWLEDGEMENTS

We are grateful to the patients, their families, physicians and the International Incontinentia Pigmenti Consortium (http://imgen.bcm.tmc.edu/IPIF/) for the valuable co-operation. In particular, we would like to thank Dr C. Ayuso (Madrid, Spain), Dr E.J. Molins (Barcelona, Spain), Dr G. Tadini (Milan, Italy), Dr R. Tenconi (Padova, Italy) and Professor V. Ventruto (Naples, Italy) for referring patients to us. For critical reading of the manuscript, we wish to thank Professor David Schlessinger. We also thank Tatiana Lopez for technical help. This work was supported by FIRB grant from MIUR and by Telethon, Italy (grant GGP02414 to M.D.), by CNR fellowship to G.F. and by BioGeM salary to T.B. and V.M.

REFERENCES

1. Landy, S.J. and Donnai, D. (1993) Incontinentia pigmenti (Bloch–Sulzberger syndrome). *J. Med. Genet.*, **30**, 53–59.
2. Yamaoka, S., Courtois, G., Bessia, C., Whiteside, S.T., Weil, R., Agou, F., Kirk, H.E., Kay, R.J. and Israel, A. (1998) Complementation cloning of NEMO, a component of the IkappaB kinase complex essential for NF-kappaB activation. *Cell*, **93**, 1231–1240.
3. Rothwarf, D.M., Zandi, E., Natoli, G. and Karin, M. (1998) IKK-gamma is an essential regulatory subunit of the IkappaB kinase complex. *Nature*, **395**, 297–300.
4. Israel, A. (2000) The IKK complex: an integrator of all signals that activate NF-kappaB? *Trends Cell Biol.*, **10**, 129–133.
5. Ghosh, S., May, M.J. and Kopp, E.B. (1998) NF-kappa B and Rel proteins: evolutionarily conserved mediators of immune responses. *Ann. Rev. Immunol.*, **16**, 225–260.
6. Karin, M. and Ben-Neriah, Y. (2000) Phosphorylation meets ubiquitination: the control of NF-[kappa]B activity. *Ann. Rev. Immunol.*, **18**, 621–663.
7. Makris, C., Godfrey, V.L., Krahn-Senftleben, G., Takahashi, T., Roberts, J.L., Schwarz, T., Feng, L., Johnson, R.S. and Karin, M. (2000) Female mice heterozygous for IKK gamma/NEMO deficiencies develop a dermatopathy similar to the human X-linked disorder incontinentia pigmenti. *Mol. Cell.*, **5**, 969–979.
8. Rudolph, D., Yeh, W.C., Wakeham, A., Rudolph, B., Nallainathan, D., Potter, J., Elia, A.J. and Mak, T.W. (2000) Severe liver degeneration and lack of NF-kappaB activation in NEMO/IKKgamma-deficient mice. *Gen. Dev.*, **14**, 854–862.
9. Schmidt-Supprian, M., Bloch, W., Courtois, G., Addicks, K., Israel, A., Rajewsky, K. and Pasparakis, M. (2000) NEMO/IKK gamma-deficient mice model incontinentia pigmenti. *Mol. Cell.*, **5**, 981–992.
10. Zonana, J., Elder, M.E., Schneider, L.C., Orlow, S.J., Moss, C., Golabi, M., Shapira, S.K., Farndon, P.A., Wara, D.W., Emmal, S.A. and Ferguson, B.M. (2000) A novel X-linked disorder of immune deficiency and hypohidrotic ectodermal dysplasia is allelic to incontinentia pigmenti and due to mutations in IKK-gamma (NEMO). *Am. J. Hum. Genet.*, **67**, 1555–1562.
11. Doffinger, R., Smahi, A., Bessia, C., Geissmann, F., Feinberg, J., Durandy, A., Bodemer, C., Kenwrick, S., Dupuis-Girod, S., Blanche, S. *et al.* (2001) X-linked anhidrotic ectodermal dysplasia with immunodeficiency is caused by impaired NF-kappaB signaling. *Nat. Genet.*, **27**, 277–285.
12. Aradhya, S., Courtois, G., Rajkovic, A., Lewis, R.A., Levy, M., Israel, A. and Nelson, D.L. (2001) Atypical forms of incontinentia pigmenti in male individuals result from mutations of a cytosine tract in exon 10 of NEMO (IKK-gamma). *Am. J. Hum. Genet.*, **68**, 765–771.
13. Smahi, A., Courtois, G., Vabres, P., Yamaoka, S., Heuertz, S., Munnich, A., Israel, A., Heiss, N.S., Klauck, S.M., Kioschis, P. *et al.* The International Incontinentia Pigmenti (IP) Consortium. (2000) Genomic rearrangement in NEMO impairs NF-kappaB activation and is a cause of incontinentia pigmenti. *Nature*, **405**, 466–472.
14. Bardaro, T., Falco, G., Sparago, A., Mercadante, V., Gean Molins, E., Tarantino, E., Ursini, M.V. and D'Urso, M. (2003) Two cases of misinterpretation of molecular results in incontinentia pigmenti, and a PCR-based method to discriminate NEMO/IKKgamma gene deletion. *Hum. Mutat.*, **21**, 8–11.
15. Aradhya, S., Woffendin, H., Jakins, T., Bardaro, T., Esposito, T., Smahi, A., Shaw, C., Levy, M., Munnich, A., D'Urso, M. *et al.* (2001) A recurrent deletion in the ubiquitously expressed NEMO (IKK-gamma) gene accounts for the vast majority of incontinentia pigmenti mutations. *Hum. Mol. Genet.*, **10**, 2171–2179.
16. Sironi, M., Pozzoli, U., Cagliani, R., Giorda, R., Comi, G.P., Bardoni, A., Menozzi, G. and Bresolin, N. (2003) Relevance of sequence and structure elements for deletion events in the dystrophin gene major hot-spot. *Hum. Genet.*, **112**, 272–288.
17. Lakich, D., Kazazian, H.H., Jr, Antonarakis, S.E. and Gitschier, J. (1993) Inversions disrupting the factor VIII gene are a common cause of severe haemophilia A. *Nat. Genet.*, **5**, 236–241.
18. Courtois, G., Whiteside, S.T., Sibley, C.H. and Israel, A. (1997) Characterization of a mutant cell line that does not activate NF-kappaB in response to multiple stimuli. *Mol. Cell. Biol.*, **17**, 1441–1449.
19. Hoshino, K., Takeuchi, O., Kawai, T., Sanjo, H., Ogawa, T.,Takeda, Y., Takeda, K. and Akira, S. (1999) Cutting edge: Toll-like receptor 4 (TLR4)-deficient mice are hyporesponsive to lipopolysaccharide: evidence for TLR4 as the LPS gene product. *J. Immunol.*, **162**, 3749–3752.
20. Busque, L., Mio, R., Mattioli, J., Brais, E., Blais, N., Lalonde, Y., Maragh, M. and Gilliland, D.G. (1996) Non random X-inactivation patterns in normal females: lyonization ratios vary with age. *Blood*, **88**, 59–65.
21. Sharp, A., Robinson, D. and Jacobs, P. (2000) Age- and tissue-specific variation of X chromosome inactivation ratios in normal women. *Hum. Genet.*, **107**, 343–349.
22. Plenge, R.M., Tranebjaerg, L., Jensen, P.K., Schwartz, C. and Willard, H.F. (1999) Evidence that mutations in the X-linked DDP gene cause incompletely penetrant and variable skewed X inactivation. *Am. J. Hum. Genet.*, **64**, 759–767.
23. Ketterling, R.P., Vielhaber, E., Bottema, C.D., Schaid, D.J., Cohen, M.P., Sexauer, C.L. and Sommer, S.S. (1993) Germ-line origins of mutation in families with hemophilia B: the sex ratio varies with the type of mutation. *Am. J. Hum. Genet.*, **52**, 152–166.
24. Valleix, S., Nafa, K., Stieltjes, N., Viemont, M., Sultan, Y., Kaplan, J.C. and Delpech, M. (1997) Prevalence, male germ-line origin and new patterns of inversions in hemophilia A. *Ann. Genet.*, **40**, 35–40.
25. Wan, M., Lee, S.S., Zhang, X., Houwink-Manville, I., Song, H.R., Amir, R.E., Budden, S., Naidu, S., Pereira, J.L., Lo, I.F. *et al.* (1999) Rett syndrome and beyond: recurrent spontaneous and familial MECP2 mutations at CpG hotspots. *Am. J. Hum. Genet.*, **65**, 1520–1529.
26. Wiegmann, K., Schutze, S., Kampen, E., Himmler, A., Machleidt, T. and Kronke, M. (1992) Human 55-kDa receptor for tumor necrosis factor coupled to signal transduction cascades. *J. Biol. Chem.*, **267**, 17997–18001.
27. Mattson, M.P. and Camandola, S. (2001) NF-kappaB in neuronal plasticity and neurodegenerative disorders. *J. Clin. Invest.*, **107**, 247–254.
28. Battaglia, A. (2003) Neuroimaging studies in the evaluation of developmental delay/mental retardation. *Am. J. Med. Genet.*, **117**, 25–30.
29. Bennett, J.L. (2002) Developmental neurogenetics and neuro-ophthalmology. *J. Neuroophthalmol.*, **22**, 286–296.

30. Jones, A.C., Austin, J., Hansen, N., Hoogendoorn, B., Oefner, P.J., Cheadle, J.P. and O'Donovan, M.C. (1999) Optimal temperature selection for mutation detection by denaturing HPLC and comparison to single-stranded conformation polymorphism and heteroduplex analysis. *Clin. Chem.*, **45**, 1133–1140.
31. Antonarakis, S.E. (1998) Recommendations for a nomenclature system for human gene mutations. Nomenclature Working Group. *Hum. Mutat.*, **11**, 1–3.
32. Mercurio, F., Zhu, H., Murray, B.W., Shevchenko, A., Bennett, B.L., Li, J.W., Young, D.B., Barbosa, M., Mann, M. and Rao, A. (1997) IKK-1 and IKK-2: cytokine-activated IkappaB kinases essential for NF-kappaB activation. *Science*, **278**, 860–866.
33. Sambrook, J., Fritsch, E.F. and Maniatis, T. (1989) *Molecular Cloning: A Laboratory Manual.* Cold Spring Laboratory Press.
34. Allen, R.C., Zoghbi, H.Y., Moseley, A.B., Rosenblatt, H.M. and Belmont, J.W. (1992) Methylation of *Hpa*II and *Hha*I sites near the polymorphic CAG repeat in the human androgen-receptor gene correlates with X-chromosome inactivation. *Am. J. Hum. Genet.*, **51**, 1229–1239.
35. Schanen, N.C., Dahle, E.J., Capozzoli, F., Holm, V.A., Zoghbi, H.Y. and Francke, U. (1997) A new Rett syndrome family consistent with X-linked inheritance expands the X-chromosome exclusion map. *Am. J. Hum. Genet.*, **61**, 634–641.
36. Hammer, S., Dorrani, N., Hartiala, J., Stein, S. and Schanen, N.C. (2003) Rett syndrome in a 47XXX patient with a *de novo* MECP2 mutation. *Am. J. Med. Genet.*, **122A**, 223–226.